

Exceptional points and phase transitions in non-Hermitian nonlinear binary systemsAmir Rahmani ¹, Andrzej Opala,^{1,2} and Michał Matuszewski ¹¹*Institute of Physics, Polish Academy of Sciences, Aleja Lotników 32/46, PL-02-668 Warsaw, Poland*²*Faculty of Physics, Institute of Experimental Physics, University of Warsaw, ulica Pasteura 5, PL-02-093 Warsaw, Poland*

(Received 4 July 2023; revised 6 November 2023; accepted 17 January 2024; published 23 February 2024)

A recent study [R. Hanai *et al.*, *Phys. Rev. Lett.* **122**, 185301 (2019)] highlighted a first-order-like dissipative phase transition in a two-component quantum system with an exceptional point coinciding with the phase boundary endpoint. Here, we show a disparity between the exceptional point and the endpoint which is closely connected to the stability of solutions. We present a general phase diagram describing different phases in a generic nonlinear binary system. The phase transition may occur also in the regime of weak coupling between the modes, which was excluded previously. In a certain range of parameters, the system converges to a limit cycle, which vanishes at the exceptional point. Our results emphasize the connection between phase transitions, bistability, and exceptional points of non-Hermitian nonlinear systems in general, providing insight into strongly coupled light-matter systems in particular.

DOI: [10.1103/PhysRevB.109.085311](https://doi.org/10.1103/PhysRevB.109.085311)**I. INTRODUCTION**

Phase transitions correspond to significant alterations of the properties of a system caused by the modification of physical parameters. Examples include the ferromagnetic-paramagnetic phase transition [1], the gas-liquid-solid transition [2], Bose-Einstein condensation in bosonic and fermionic systems [3], the metal-insulator transition in the solid state [4], and topological phase transitions [5]. Phase transitions may also occur in non-Hermitian systems, which are systems that do not satisfy the condition of Hermiticity, which is embedded in quantum mechanics [6]. Here, the non-Hermitian contributions may stem from dissipation [7] or asymmetric coupling [8] and lead to a number of unique properties such as nonreciprocity [9], mutually interlinked non-Hermitian phase transitions [10], and the non-Hermitian skin effect [11].

A striking example of non-Hermitian physics that deviates significantly from the Hermitian case is the coalescence of eigenstates and energy eigenvalues at so-called exceptional points (EPs). These are different from Hermitian singularities, such as diabolical points, where some of the eigenvalues may coalesce while corresponding eigenvectors remain orthogonal. Exceptional points may be accompanied by a non-Hermitian phase transition in the case of nonresonant pumping [12] or a topological phase transition [13,14]. The standard procedure to investigate these phase transitions is through the study of the spectrum of the system as some controllable parameters are changed [7]. Typically, the process involves the meticulous adjustment of loss and gain in order to achieve the desired outcome. In general, in a linear system the presence of EPs is independent of the stability of the stationary state to which the system evolves [15]. However, in a nonlinear system, more than one solution may be stable, which gives rise to the phenomena of bistability and multistability [16–19]. The existence of nonlinear features may affect the non-Hermitian effects realized in linear cases or give rise to entirely new phenomena [20–27].

In order to examine the relationship between nonlinearity and non-Hermitian physics, it is necessary to study systems that possess variable nonlinearity and controllable gain and loss. Particularly suitable systems for this study are those where matter couples with light, as they allow to take advantage of the difference in the physical properties of these components. For example, it was demonstrated that exceptional points appear naturally in light-matter systems of exciton polaritons and subthreshold Fabry-Pérot lasers [15,28]. Moreover, it is possible to induce exceptional points by manipulating spatial and spin degrees of freedom of exciton polaritons in various configurations [21,29–39]. In the case of bosonic condensates of exciton polaritons, it was predicted that a dissipative first-order-like phase transition line exists in the phase diagram [28], similar to a critical point in a liquid-gas phase transition. According to this study, this phase transition line exists in the regime of strong light-matter coupling and has an endpoint which corresponds to an exceptional point [28].

In this paper, we investigate a non-Hermitian binary model with nonresonant pumping, accentuating the significance of nonlinearity in a non-Hermitian phase transition. This minimal model can describe a wide range of physical systems, including simple coupled oscillating modes, but also allows to describe two-component homogeneous systems in the thermodynamic limit of large volume and large particle numbers. In particular, it describes the light and matter interaction in exciton-polariton condensation and lasing, as investigated in Ref. [28]. We note that a separate line of research is devoted to resonantly driven light-matter systems with a coherent forcing term [40–45], which differ essentially from our model. We find that the model under investigation is incomplete unless the nonlinear saturation of gain is taken into account. Importantly, saturation increases the complexity of the phase diagram and leads to the appearance of bistability. We find that while the first-order-like phase transition line with an endpoint is present, the equivalence of the endpoint to an

exceptional point as found in Ref. [28] is no longer valid in the general case. The phase diagram of Ref. [28] can be restored in the limit of strong saturation, but the transition can occur also in the weak-coupling regime. This suggests that the second threshold from polariton to photon lasing, observed in experiments [46–48], may be related to a dissipative phase transition in the weak-coupling regime. Moreover, we find a regime of limit cycle solutions due to a Hopf bifurcation, which eventually disappear at an exceptional point.

II. MODEL AND ANALYTICAL SOLUTIONS

We consider a two-mode anharmonic system described by a non-Hermitian Hamiltonian with gain and loss, in the absence of resonant forcing terms. The imbalance between gain and loss in a linear system leads in general to solutions exponentially growing or decaying in time. To obtain nontrivial stationary solutions it is necessary to include nonlinearity. Here, we adopt cubic nonlinearity that appears naturally in symmetric systems with no dependence on the complex phase. Such a model can be realized, for instance, in a microcavity [49] or a coplanar waveguide [50]. The system is described by complex functions $\psi_C = n_C e^{i\varphi_C}$ and $\psi_X = n_X e^{i\varphi_X}$. We may refer to those fields respectively as cavity photons and excitons in the case of a microcavity, however, they can be assigned to any physical modes as long as one of them (C) experiences loss and the other one experiences saturable gain and nonlinearity (X). The dynamics is governed by equations $i\hbar\partial_t|\Psi\rangle = H|\Psi\rangle$ with $|\Psi\rangle = (\psi_C, \psi_X)^T$, where the non-Hermitian Hamiltonian H is given by [28]

$$H = \begin{pmatrix} E_C - i\hbar\gamma_C & \hbar\Omega_R \\ \hbar\Omega_R & E_X + g|\psi_X|^2 + ip \end{pmatrix}. \quad (1)$$

Here, $\hbar\Omega_R$ is the coupling strength, γ_C is the decay rate of the photon field, and p represents the gain to the exciton field. This gain can be realized in practice by nonresonant optical or electrical pumping. We note that the above description does not explicitly include the incoherent reservoir, which is justified under certain conditions such as the separation of timescales for the reservoir and polaritons [51]. We define the complex nonlinear coefficient as $g = g_1 - ig_2$, where g_1 is the strength of Kerr-like nonlinearity and $g_2|\psi_X|^2$ is the saturation term. The spectrum of Hamiltonian (1) is

$$E = \frac{1}{2}[E_c + \mathcal{E} + i(\mathcal{P} - \hbar\gamma_c)] \pm \sqrt{4\hbar^2\Omega_R^2 + [\mathcal{E} - E_c + i(\mathcal{P} + \hbar\gamma_c)]^2}, \quad (2)$$

where $\mathcal{P} = p - g_2(n_X^{SS})^2$ and $\mathcal{E} = E_x + g_1(n_X^{SS})^2$. For convenience, we denote the solution associated with plus (minus) by U (L). The respective steady state analytical solutions $|\Psi\rangle = |\Psi_0\rangle e^{-iEt}$ can be found from the condition $\text{Im}[E] = 0$. In Ref. [28], it was argued that one or two real-energy solutions exist in certain regions in parameter space. However, it can be seen from (2) that except from special values of the parameters, real-energy solutions can exist only when saturation represented by g_2 is taken into account. We will show below that accounting for the nonlinear g_2 term does in fact lead to the appearance of up to three real-energy solutions, each of

them of the form (2). The condition $\text{Im}[E] = 0$ allows one to find analytical expression for n_X^{SS} ,

$$(n_X^{SS})^2 = \frac{1}{g} \left(\text{Re}[E] - E_X - iP - \frac{(\hbar\Omega_R)^2}{\text{Re}[E] - E_C + i\hbar\gamma_C} \right). \quad (3)$$

The resulting explicit formula for n_X^{SS} is tedious, but for a given n_X^{SS} , one can find closed forms of steady state n_C^{SS} and $\varphi_{CX} = \varphi_C - \varphi_X$,

$$n_C^{SS} = n_X^{SS} \sqrt{\frac{p}{\hbar\gamma_C} - \frac{(n_X^{SS})^2 g_2}{\hbar\gamma_C}}, \quad (4)$$

$$\varphi_{CX}^{SS} = \arg \left(\frac{\delta - g_1(n_X^{SS})^2}{\hbar\Omega_R(n_C^{SS}/n_X^{SS} - n_X^{SS}/n_C^{SS})} - i \frac{\gamma_C n_C^{SS}}{\Omega_R n_X^{SS}} \right), \quad (5)$$

where we introduced photon-exciton energy detuning $\delta = E_C - E_X$.

III. RESULTS AND DISCUSSION

A. Non-Hermitian first-order-like phase transitions

We use the analytical solutions from the previous section to determine the phase diagram. We analyze steady state solutions and their multiplicity in Fig. 1(a). Additionally, we consider the lowest-energy state among the dynamically stable ones [see Fig. 1(b)]. The latter is equivalent to adding a weakly coupled energy sink, which does not perturb the spectrum, but picks the lowest-energy stable solution due to its energetic stability.

In the case when the conservative nonlinearity g_1 is stronger than the dissipative nonlinearity g_2 , representative phase diagrams are shown in Fig. 1. We focus on the blue-detuned case ($\delta > 0$), which is much richer than the red-detuned case. In Fig. 1(a) the number of steady state solutions is shown. Up to three nonzero solutions, corresponding to both the upper and lower branches of Eq. (2), can exist, which results from the nonlinearity of the system. The region of zero solutions corresponds to the situation where pumping cannot overcome losses and no lasing nor polariton condensation occurs. For a given Ω and γ_C , increasing pumping p can lead to one or several thresholds, as indicated with horizontal lines.

Special points in the phase diagram (marked by stars in Fig. 1) include the exceptional point (EP) and the endpoint of the first-order-like phase transition (ET). In contrast to Ref. [28], we find that in general they do not coincide. Analyzing the eigenvalues in Eq. (2), one can find the following conditions for the EP,

$$p^{\text{EP}} = \hbar\Omega_R + \frac{g_2\delta}{g_1}, \quad \gamma_C = \Omega_R. \quad (6)$$

This can occur when $n_X^{SS} = \sqrt{\delta/g_1}$, that is, whenever the system is blue detuned ($\delta > 0$). On the other hand, the ET point is clearly visualized in the phase diagram that takes into account the energetic instability in Fig. 1(b). The first-order-like phase transition line begins at the ET point in the weak-coupling regime ($\gamma_C > \Omega_R$) and follows the arc represented by the ET-EP line towards the EP point. Below the EP, the phase transition line follows into the strong-coupling regime. We conclude that, contrary to the results of Ref. [28],

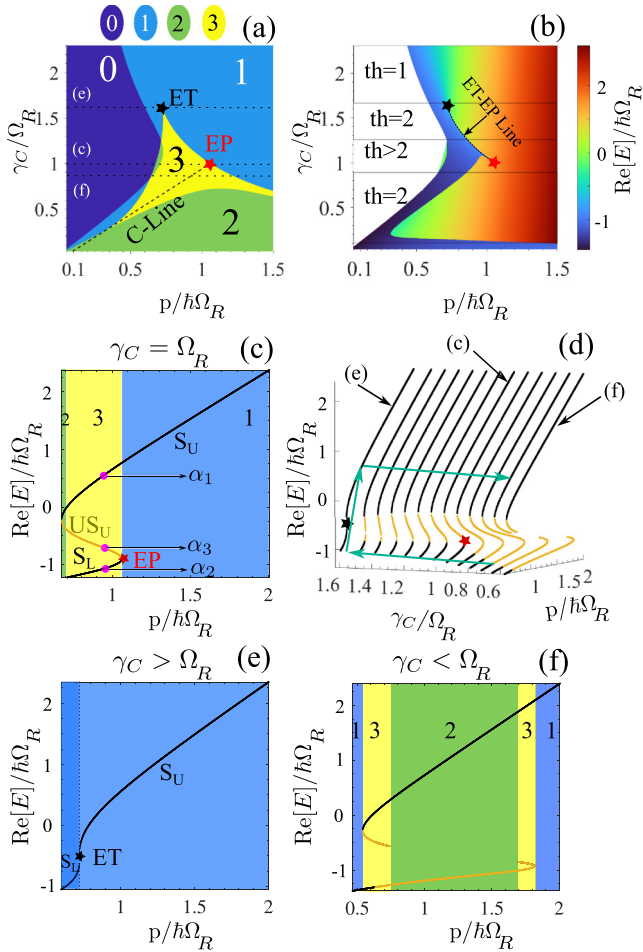


FIG. 1. (a), (b) Phase diagrams of binary system (1). In (a), the number of stationary states is marked with colors in the function of photon decay rate (γ_c) and pumping strength (p). In (b), only the lowest-energy stable state is shown. Here, colors indicate the real part of the energy. In (a) and (b), the exceptional point (EP, red star) and the endpoint of the first-order-like phase transition (ET) are shown. At the C-line two solutions coalesce and the periodic solution vanishes. Cross sections of constant γ_c with different numbers of thresholds (th) are marked with horizontal lines. In (c), we show the case $\gamma_C = \Omega_R$, for which the energy eigenvalues coalesce at the EP. Stable solutions are marked with S and black lines, while unstable solutions are marked with US and orange lines. (d) shows the real part of energy for different pumping and decay rates. The ET point corresponds to the transition to bistability at $\gamma_C > \Omega_R$. This cross section is depicted in (e), while in (f) we show the case $\gamma_C < \Omega_R$, where the unstable solution is split into two branches, and the lowest-energy solution becomes unstable. Other parameters are [52] $\delta = 0.2\hbar\Omega_R$, $g_1 = 0.1\hbar\Omega_R$, $E_X = 0$, $E_C = 0.2\hbar\Omega$, and $g_2 = 0.3g_1$.

the first-order-like phase transition can occur also in the weak-coupling regime. This can be explained by a simple physical argument. Since the pumping influences the effective detuning between modes $\delta = E_C - [E_X + g(n_X^{SS})^2]$, the increase of pumping can change of the sign of δ , leading to an abrupt change of the lowest-energy state in the weak-coupling regime.

Figure 1(d) shows the dependence of the real part of the energy of solutions shown in Figs. 1(a) and 1(b), in the

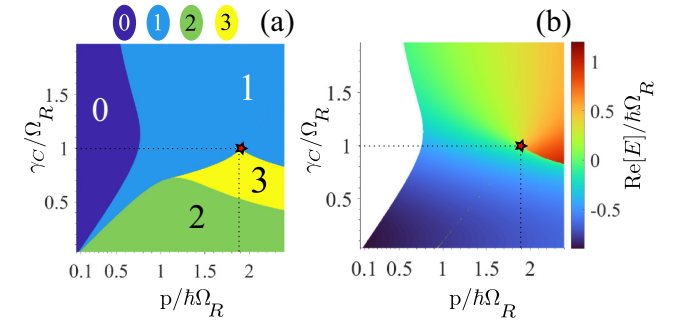


FIG. 2. Phase diagrams in the case when dissipative nonlinearity g_2 dominates over the conservative nonlinearity g_1 . The endpoint of the phase transition (ET) and the exceptional point (EP) coincide, recovering the results of Ref. [28]. Parameters as in Fig. 1, except for $g_2 = 4.5g_1$.

vicinity of the ET-EP line. As can be seen, the ET point is the point of the transition to bistability. On the other hand, the EP point corresponds to a turning point in the bistability curve. The cross section including the EP point ($\gamma_C = \Omega$) is depicted in more detail in Fig. 1(c), which shows the occurrence of two stable branches from the upper and lower branches of Eq. (2) and one unstable branch. At the EP, the unstable upper branch coalesces with the lower stable branch, leading to the first-order-like phase transition. The cross section with the ET point ($\gamma_C > \Omega_R$) is shown in Fig. 1(e), where the bistability curve closes, and the transition from the upper to lower branch becomes smooth. This leads to the possibility to encircle the exceptional point, as indicated with arrows in Fig. 1(d).

Interestingly, additional features that have an influence on the physics of the system can occur in the strong-coupling case ($\gamma_C < \Omega_R$) [see Fig. 1(f)]. These include the disappearance of one of the solutions in a certain parameter range and the dynamical instability of the lowest-energy branch (marked with an orange line). Consequently, the upper, higher-energy solution may become the only stable solution.

In the opposite case when the dissipative nonlinearity g_2 dominates over the conservative one g_1 , we find that the phase diagram of energetically stable solutions recovers the results of Ref. [28] (see Fig. 2). As the dissipative nonlinearity is increased, the length of the ET-EP arc decreases, and finally the two points coalesce. In this specific case, the exceptional point is characterized by a jagged crest in the phase diagram, embodying a third-order exceptional point (see Supplemental Material [53]).

B. Permanent oscillations

Our analysis allows to predict that a peculiar oscillating state may form next to the coalescence line (C-line) in Fig. 1(a). In this case, long evolution leads to periodic oscillations, or a limit cycle, instead of stationary solutions. To explain this phenomenon, we examine Jacobian eigenvalues of linear stability (denoted by λ) given in the Supplemental Material [53]. Examples are shown in Figs. 3(a) and 3(b). In close proximity to the C-line [$p_C = (g_2/g_1)\delta + \hbar\gamma_C$] the stability of the steady state changes. As we approach p_C , the only stable solution becomes unstable, as two complex eigenvalues cross the imaginary axis in the Argand map [Fig. 3(b)], and a

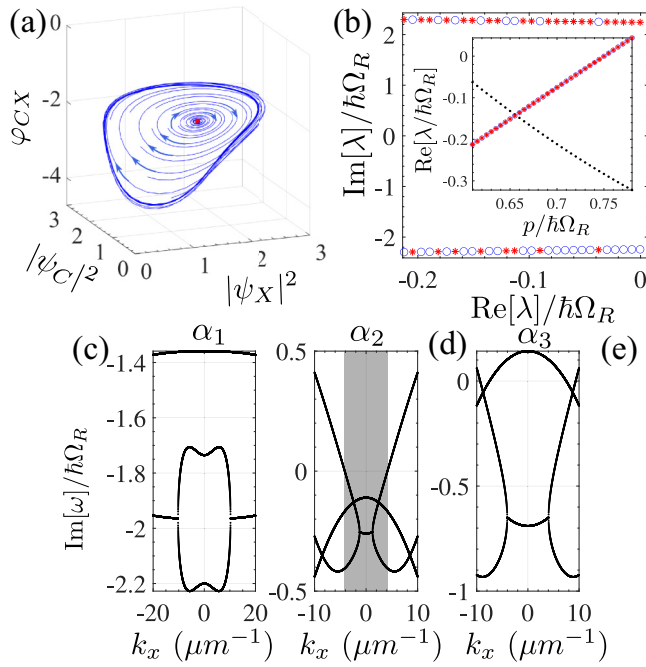


FIG. 3. (a) Example of oscillations converging to a limit cycle. The red point is the initial condition that is close to an unstable fixed point. (b) Argand map of Jacobian eigenvalues of fixed points. As the real part crosses the zero axis, oscillations appear. [(c)–(e)] Imaginary part of the spectra of elementary excitations corresponding to three points ($\alpha_{i=1,2,3}$) in Fig. 1(c). [(c)–(e)] correspond to α_1 , α_2 , and α_3 , respectively. The stability region in (d) is marked in gray. Parameters are $p = 0.775\hbar\Omega_R$, $\gamma_C = 0.75\Omega_R$, $g_1 = 0.1\hbar\Omega_R$, $g_2 = 0.3g_1$, and $\delta = 0.2\hbar\Omega_R$.

periodic solution emerges (see Supplemental Material [53] for more details). This oscillation is due to Hopf bifurcation [54]. As shown in Fig. 3(a), the fixed point is unstable and the blue trajectory converges to the stable orbit. The frequency of oscillations can be approximated by the gap in the complex plane shown in Fig. 3(b), that is, $\hbar\Omega = 2 \text{Im}[\lambda_0]$ with $\text{Re}[\lambda_0] = 0$. At $p = p_C$, the periodic solution dies out and the solutions coalesce to a single point with $n_C^{\text{SS}} = n_X^{\text{SS}} = \sqrt{\delta/g_1}$ and $\varphi_{CX} = \sin^{-1}[-\gamma_C/\Omega]$. When the parameters of the system approach the exceptional point ($\Omega_R = \gamma_C$) the two solutions meet at a stable point. Therefore, the exceptional point is the endpoint of the C -line. In other words, the C -line is where the oscillatory solutions vanish. At the EP, the system has only one, stable, degenerate solution.

C. Spatial fluctuations

Our model can describe both simple, discrete binary systems, and extended homogeneous systems in the

thermodynamic limit. In the latter case, nonlinearity may give rise to elementary excitations, which may be of a classical or quantum [55] nature. Such fluctuations can be analyzed via linearization around the steady state and plane-wave expansion, $\psi_j = \psi_j^{\text{SS}} + \epsilon(u_j e^{ik_x x} + v_j^* e^{-ik_x x})$, where $j = C, X$. Keeping terms linear in ϵ , the dynamics of fluctuations $\delta\psi = (u_X, u_C, v_X^*, v_C^*)^T$ follow $i\hbar\partial_t \delta\psi = \mathcal{L}\delta\psi$, where \mathcal{L} is given in the Supplemental Material [53]. The imaginary parts of eigenvalues of \mathcal{L} , denoted by ω , are shown in the lower panels of Fig. 3, for three points in the bistable regime as marked by $\alpha_{i=1,2,3}$ in Fig. 1(c). The solutions corresponding to α_1 and α_2 are stable against spatial fluctuations if $\text{Im}[\omega] < 0$. One can see that the fluctuations of the lower-branch α_2 solution are not stable at high momentum. Therefore, this solution may be stable only in the case when additional effects that suppress these high-momentum modes come into play, such as energy relaxation [56].

IV. CONCLUSION

We showed that, contrary to previous understandings, non-Hermitian two-mode systems exhibit a first-order-like dissipative phase transition with an endpoint that in general does not coincide with the exceptional point. While the endpoint is where the bistability appears, the exceptional point is where the stable and unstable solutions coalesce. We demonstrated that a first-order-like phase transition may occur in the weak-coupling regime, and that for certain values of parameters one can predict oscillatory solutions, which converge to a stable exceptional point.

The predicted results contribute to the ongoing debate surrounding polariton/photon lasing in a nonlinear polariton system. The presented results are also applicable to a much broader class of systems. The non-Hermitian Hamiltonian in Eq. (1) describes an arbitrary two-mode nonlinear system with gain and loss in the two modes, and the cubic nonlinearity in one of them. This term appears naturally in any oscillatory system in the first order as long as it respects the global $U(1)$ symmetry. Examples include systems such as Bose-Einstein condensates, high-frequency coupled classical oscillators, where the phase of oscillations is irrelevant on the timescale of a slowly varying envelope.

ACKNOWLEDGMENTS

A.R. and M.M. acknowledge support from National Science Center, Poland (PL), Grant No. 2016/22/E/ST3/00045. A.O. acknowledges support from National Science Center, Poland (PL), Grant No. 2019/35/N/ST3/01379 and Foundation for Polish Science (FNP).

[1] D. Jiles, *Introduction to Magnetism and Magnetic Materials* (CRC Press, Boca Raton, FL, 2015).
 [2] S. M. Stishov, *Phase Transitions for Beginners* (World Scientific, Singapore, 2018).
 [3] N. Proukakis, D. Snoke, and P. Littlewood, *Universal Themes of Bose-Einstein Condensation* (Cambridge University Press, Cambridge, UK, 2017).

[4] M. Imada, A. Fujimori, and Y. Tokura, *Rev. Mod. Phys.* **70**, 1039 (1998).
 [5] L. Brink, M. Gunn, J. Jose, J. Kosterlitz, and K. Phua, *Topological Phase Transitions and New Developments* (World Scientific, Singapore, 2018).
 [6] Y. Ashida, Z. Gong, and M. Ueda, *Adv. Phys.* **69**, 249 (2020).
 [7] M.-A. Miri and A. Alù, *Science* **363**, eaar7709 (2019).

- [8] Z. Gong, Y. Ashida, K. Kawabata, K. Takasan, S. Higashikawa, and M. Ueda, *Phys. Rev. X* **8**, 031079 (2018).
- [9] B. Peng, S. K. Ozdemir, F. Lei, F. Monifi, M. Gianfreda, G. L. Long, S. Fan, F. Nori, C. M. Bender, and L. Yang, *Nat. Phys.* **10**, 394 (2022).
- [10] S. Weidemann, M. Kremer, S. Longhi, and A. Szameit, *Nature (London)* **601**, 354 (2022).
- [11] N. Okuma and M. Sato, *Annu. Rev. Condens. Matter Phys.* **14**, 83 (2023).
- [12] F. E. Öztürk, T. Lappe, G. Hellmann, J. Schmitt, J. Klaers, F. Vewinger, J. Kroha, and M. Weitz, *Science* **372**, 88 (2021).
- [13] A. A. Mailybaev, O. N. Kirillov, and A. P. Seyranian, *Phys. Rev. A* **72**, 014104 (2005).
- [14] C. Dembowski, B. Dietz, H.-D. Gräf, H. L. Harney, A. Heine, W. D. Heiss, and A. Richter, *Phys. Rev. E* **69**, 056216 (2004).
- [15] J. B. Khurgin, *Optica* **7**, 1015 (2020).
- [16] R. W. Boyd, *Nonlinear Optics* (Academic Press, London, 2020).
- [17] T. Paraiso, M. Wouters, Y. Léger, F. Morier-Genoud, and B. Deveaud-Plédran, *Nat. Mater.* **9**, 655 (2010).
- [18] N. A. Gippius, I. A. Shelykh, D. D. Solnyshkov, S. S. Gavrilov, Y. G. Rubo, A. V. Kavokin, S. G. Tikhodeev, and G. Malpuech, *Phys. Rev. Lett.* **98**, 236401 (2007).
- [19] E. Cancellieri, F. M. Marchetti, M. H. Szymańska, and C. Tejedor, *Phys. Rev. B* **83**, 214507 (2011).
- [20] Z.-F. Yu, J.-K. Xue, L. Zhuang, J. Zhao, and W.-M. Liu, *Phys. Rev. B* **104**, 235408 (2021).
- [21] J. Wingenbach, S. Schumacher, and X. Ma, [arXiv:2305.04855](https://arxiv.org/abs/2305.04855).
- [22] S. Ramezanpour and A. Bogdanov, *Phys. Rev. A* **103**, 043510 (2021).
- [23] S. Xia, D. Kaltsas, D. Song, I. Komis, J. Xu, A. Szameit, H. Buljan, K. G. Makris, and Z. Chen, *Science* **372**, 72 (2021).
- [24] A. U. Hassan, H. Hodaie, M.-A. Miri, M. Khajavikhan, and D. N. Christodoulides, *Phys. Rev. A* **92**, 063807 (2015).
- [25] H. Ramezani, T. Kottos, R. El-Ganainy, and D. N. Christodoulides, *Phys. Rev. A* **82**, 043803 (2010).
- [26] R. El-Ganainy, K. G. Makris, M. Khajavikhan, Z. H. Musslimani, S. Rotter, and D. N. Christodoulides, *Nat. Phys.* **14**, 11 (2018).
- [27] M. Wimmer, A. Regensburger, M.-A. Miri, C. Bersch, D. N. Christodoulides, and U. Peschel, *Nat. Commun.* **6**, 7782 (2015).
- [28] R. Hanai, A. Edelman, Y. Ohashi, and P. B. Littlewood, *Phys. Rev. Lett.* **122**, 185301 (2019).
- [29] T. Gao, G. Li, E. Estrecho, T. C. H. Liew, D. Comber-Todd, A. Nalitov, M. Steger, K. West, L. Pfeiffer, D. W. Snoke, A. V. Kavokin, A. G. Truscott, and E. A. Ostrovskaya, *Phys. Rev. Lett.* **120**, 065301 (2018).
- [30] Y. Li, X. Ma, Z. Hatzopoulos, P. G. Savvidis, S. Schumacher, and T. Gao, *ACS Photonics* **9**, 2079 (2022).
- [31] M. Król, I. Septembre, P. Oliwa, M. Kędziora, K. Łempicka-Mirek, M. Muszyński, R. Mazur, P. Morawiak, W. Piecek, P. Kula *et al.*, *Nat. Commun.* **13**, 5340 (2022).
- [32] T. Gao, E. Estrecho, K. Bliokh, T. Liew, M. Fraser, S. Brodbeck, M. Kamp, C. Schneider, S. Höfling, Y. Yamamoto *et al.*, *Nature (London)* **526**, 554 (2015).
- [33] R. Su, E. Estrecho, D. Biegańska, Y. Huang, M. Wurdack, M. Pieczarka, A. G. Truscott, T. C. H. Liew, E. A. Ostrovskaya, and Q. Xiong, *Sci. Adv.* **7**, eabj8905 (2021).
- [34] H. G. Song, M. Choi, K. Y. Woo, C. H. Park, and Y.-H. Cho, *Nat. Photon.* **15**, 582 (2021).
- [35] R. Hanai and P. B. Littlewood, *Phys. Rev. Res.* **2**, 033018 (2020).
- [36] A. Rahmani, M. Kędziora, A. Opala, and M. Matuszewski, *Phys. Rev. B* **107**, 165309 (2023).
- [37] A. Opala, M. Furman, M. Król, R. Mirek, K. Tyszka, B. Serebyński, W. Pacuski, J. Szczytko, M. Matuszewski, and B. Piętka, [arXiv:2306.01366](https://arxiv.org/abs/2306.01366).
- [38] W. Gao, X. Li, M. Bamba, and J. Kono, *Nat. Photon.* **12**, 362 (2018).
- [39] Q. Liao, C. Leblanc, J. Ren, F. Li, Y. Li, D. Solnyshkov, G. Malpuech, J. Yao, and H. Fu, *Phys. Rev. Lett.* **127**, 107402 (2021).
- [40] W. Casteels, R. Fazio, and C. Ciuti, *Phys. Rev. A* **95**, 012128 (2017).
- [41] A. Le Boité, G. Orso, and C. Ciuti, *Phys. Rev. Lett.* **110**, 233601 (2013).
- [42] M. Foss-Feig, P. Niroula, J. T. Young, M. Hafezi, A. V. Gorshkov, R. M. Wilson, and M. F. Maghrebi, *Phys. Rev. A* **95**, 043826 (2017).
- [43] T. Fink, A. Schade, S. Höfling, C. Schneider, and A. Imamoglu, *Nat. Phys.* **14**, 365 (2018).
- [44] S. R. K. Rodriguez, W. Casteels, F. Storme, N. Carlon Zambon, I. Sagnes, L. Le Gratiet, E. Galopin, A. Lemaître, A. Amo, C. Ciuti, and J. Bloch, *Phys. Rev. Lett.* **118**, 247402 (2017).
- [45] J. M. Fink, A. Dombi, A. Vukics, A. Wallraff, and P. Domokos, *Phys. Rev. X* **7**, 011012 (2017).
- [46] J. Hu, Z. Wang, S. Kim, H. Deng, S. Brodbeck, C. Schneider, S. Höfling, N. H. Kwong, and R. Binder, *Phys. Rev. X* **11**, 011018 (2021).
- [47] M. Pieczarka, D. Biegańska, C. Schneider, S. Höfling, S. Klembt, G. Sek, and M. Syperek, *Opt. Express* **30**, 17070 (2022).
- [48] J.-S. Tempel, F. Veit, M. Aßmann, L. E. Kreilkamp, A. Rahimi-Iman, A. Löffler, S. Höfling, S. Reitzenstein, L. Worschech, A. Forchel, and M. Bayer, *Phys. Rev. B* **85**, 075318 (2012).
- [49] A. V. Kavokin, J. J. Baumberg, G. Malpuech, and F. P. Laussy, *Microcavities* (Oxford University Press, Oxford, UK, 2016).
- [50] B. Bhoi, B. Kim, S.-H. Jang, J. Kim, J. Yang, Y.-J. Cho, and S.-K. Kim, *Phys. Rev. B* **99**, 134426 (2019).
- [51] N. Bobrovska and M. Matuszewski, *Phys. Rev. B* **92**, 035311 (2015).
- [52] For realistic parameters one may use $\hbar\Omega$ between a few to hundreds of meV, corresponding to Rabi splitting in exciton-polariton systems.
- [53] See Supplemental Material at <http://link.aps.org/supplemental/10.1103/PhysRevB.109.085311> for more details on stability analysis and phase diagram at large g_2 .
- [54] S. H. Strogatz, *Nonlinear Dynamics and Chaos* (CRC Press Boca Raton, FL, 2015).
- [55] A. J. Leggett, *Rev. Mod. Phys.* **73**, 307 (2001).
- [56] M. Wouters, T. C. H. Liew, and V. Savona, *Phys. Rev. B* **82**, 245315 (2010).